JOC The Journal of Organic Chemistry

Article

pubs.acs.org/joc

Matsutakone and Matsutoic Acid, Two (Nor)steroids with Unusual Skeletons from the Edible Mushroom *Tricholoma matsutake*

Zhen-Zhu Zhao,[‡,§,⊥] He-Ping Chen,[†,‡,⊥] Bin Wu,[†] Ling Zhang,[‡] Zheng-Hui Li,[†] Tao Feng,[*,†] and Ji-Kai Liu[*,†]

[†]School of Pharmaceutical Sciences, South-Central University for Nationalities, Wuhan 430074, P. R. China

[‡]State Key Laboratory of Phytochemistry and Plant Resources in West China, Kunming Institute of Botany, Chinese Academy of Sciences, Kunming 650201, P. R. China

[§]University of Chinese Academy of Sciences, Beijing 100049, P. R. China

Supporting Information

ABSTRACT: Matsutakone (**1**), a novel sterol with an unprecedented polycyclic ring system, together with a new norsteroid matsutoic acid (**2**) were isolated from the fruiting bodies of *Tricholoma matsutake*. Their structures and absolute configurations were assigned by extensive spectroscopic analyses and computational methods. Bioassay results showed that compounds **1** and **2** exhibited inhibitory activities against acetylcholinesterase (IC_{50} 20.9 μM for **1**).

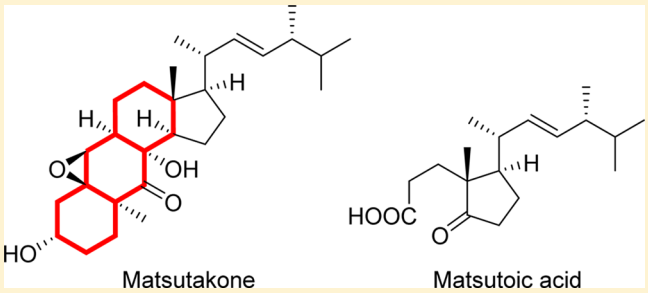

INTRODUCTION

Mushrooms are a rich source of natural products (NPs) featured by sophisticated skeletons and/or promising bioactivities.[1] Vibralactone and vibralactoximes were pancreatic lipase inhibitors with β-lactone group isolated from the fermentation broth of the fungus *Boreostereum vibrans*.[2] Hexacyclinol and panepophenanthrin were two meroterpenoids with intriguing complicated structures, remarkable cyctoxicities, and enzyme inhibitory activities derived from cultures of basidiomycete *Panus rudis*.[3] Relatively speaking, due to the high prevalence and abundance of sterols from mushroom fruiting bodies and submerged fermentations, mushroom-derived sterols have been overlooked compared to the terpenoids, meroterpenoids, and alkaloids. Whereas, mushroom originated steroids also displayed pronounced bioactivities. Strophasterols A–D were four sterols with unprecedented skeletons isolated from the mushroom *Stropharia rugosoannulata*.[4] Biological evaluation revealed that strophasterol A could protect neuronal cells by attenuating the ER stress caused by thapsigargin (TG), a Ca^{2+}-ATPase inhibitor.

The mycorrhizal fungus *Tricholoma matsutake* is a kind of incredibly delicious and nutritious wild mushroom which forms a symbiotic relationship with the roots of pine and oak trees. In summertime, the dishes of matsutake were extremely popular among Chinese dining tables. The geographical distribution of *T. matsutake* in China mainly involved in Jilin, Heilongjiang, Yunnan Provinces and Tibet Autonomous Region. Previous studies showed that the major contents of *T. matsutake* were crude fat, protein, and polysaccharides.[5] *T. matsutake* extracts displayed certain antioxidant effects on aging mice induced by D-galaction,[6] and the polysaccharides could promote the growth of lactic acid bacteria and thus improve yogurt quality.[7]

However, few of the secondary metabolites have been reported from *T. matsutake*. We herein report a chemical investigation on NPs of *T. mastutake* aiming at discovering potential drug leads led to the isolation of two novel steroids (**1**–**2**, Figure 1) and one known steroid (**3**). It was noteworthy

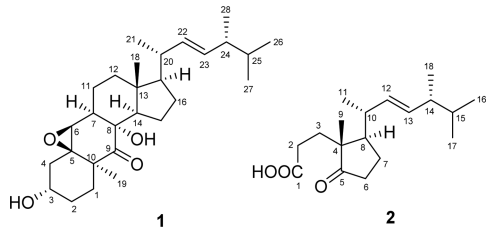

Figure 1. Structure of matsutakone (**1**) and matsutoic acid (**2**).

that compound **1** represented a new class of steroid harboring an unprecedented polycyclic system. Bioassay results indicated that compounds **1**–**2** exhibited inhibitory activities against acetylcholinesterase (AChE), an important target in the treatment of neurodegenerative diseases.

The ethyl acetate layer of *T. matsutake* (2.0 kg) was fractionated and purified by repeated chromatographic methods to yield **1** (1.4 mg), **2** (2.5 mg), and **3** (5.5 mg).

Received: May 18, 2017
Published: July 10, 2017

DOI: 10.1021/acs.joc.7b01230
J. Org. Chem. 2017, 82, 7974–7979

RESULTS AND DISCUSSION

The white powder matsutakone (**1**) was assigned the chemical formula $C_{28}H_{44}O_4$ (seven degrees of unsaturation) by a positive HRMS (ESI-TOF) experiment *m/z*: $[M + Na]^+$ calcd for $C_{28}H_{44}O_4Na$ 467.3132; found 467.3121. The ^1H NMR as well as HSQC spectra of **1** recorded in $CDCl_3$ displayed high-field signals for two methyl singlets at δ_H 0.68 (Me-18) and 1.51 (Me-19); four methyl doublets at δ_H 0.99 (Me-21), 0.82 (Me-26), 0.83 (Me-27), 0.91 (Me-28), two typical *E* double bond protons at δ_H 5.14 (dd, *J* = 15.0, 8.5 Hz, H-22), and δ_H 5.22 (dd, *J* = 15.0, 8.0 Hz, H-23), two oxygenated methines at δ_H 3.98 (m, H-3) and δ_H 3.21 (d, *J* = 4.0 Hz, H-6). The ^{13}C and DEPT spectra showed 28 carbon resonances, which were ascribed to six methyls, seven methylenes, 10 methines (two oxygenated), and five quaternary carbons (two oxygenated, one keto-carbonyl) (Table 1). Preliminary analyses of these spectroscopic features implied that **1** was a steroid, especially based on the methyl multiplicity and the typical sterol olefinic protons for *E*-form double bond of the side chain.

The $^1H-^1H$ COSY correlations of **1** readily delineated three isolated proton spin systems: H-1 to H-4, H-6/H-7/H-11/H-12, and H-15/H-16/H-17/H-20 (H-20/H_3-21)/H-22/H-23/H-24 (H-24/H_3-28)/H-25 (H-25/H_3-27)/H_3-26 (Figure 2). The HMBC correlations from H-6 to C-4 (δ_C 38.1), C-5 (δ_C 68.8), C-8 (δ_C 76.0), and C-10 (δ_C 46.3) and from Me-19 to C-1 (δ_C 29.3), C-5, C-9 (δ_C 211.1), and C-10 suggested that rings A and B were fused by sharing the C5−C10 carbon bond (Figure 2). Likewise, the HMBC correlations from angular methyl group Me-18 to C-12 (δ_C 39.2), C-13 (δ_C 43.4), C-14 (δ_C 59.0), and C-17 (δ_C 56.8), from H-15 (δ_H 2.12; 1.46) to C-14, C-8, and from H-11 (δ_H 1.75; 1.75) to C-8 allowed the formation of rings B, C, and D and also indicated that the fused manner by sharing the C7−C8 and C13−C14 carbon bonds for rings B/C and C/D, respectively. This was further supported by the key HMBC correlations from 8-OH (δ_H 1.87, s) to C-7, C-8, C-9, and C-14 (Figures S10 and S11, Supporting Information). The aforementioned assignments accounted for six double-bond equivalences. Thus, the remaining one degree of unsaturation suggested the presence of an epoxy group, which should be assigned between C-5 and C-6 in consequence of the remarkable upfield-shifted chemical shifts of C-5 (δ_C 68.8) and C-6 (δ_C 62.8) compared to corresponding oxygenated quaternary carbons and methines. Therefore, the planar structure of **1** was deduced as shown in Figure 1 and designated the name matsutakone.

The relative configuration of compound **1** was determined via ROESY experiment. The ROESY cross peaks of H-6/H-7/H-12*α*, H-7/H-14/H-17, and H-12*β*/Me-18/H-20 indicated that H-6, H-7, H-14, and H-17 were *α*-oriented, while Me-18 was *β*-oriented. Besides, the *α*-orientations of 3-OH, Me-19, and 8-OH were established by correlations of H-6/H-4*β*/H-3/H-2*β*/H-1*β*, and Me-19/H-2*α*, Me-19/H-4*α*, and Me-19/8-OH (Figure S13, Supporting Information).

To the best of our knowledge, natural ergosteroids characterized as 20*R*, 24*R* were quite common.[8] Hence, by comparing the chemical shifts of the side chain with those of ergosta-7,22-dien-5*α*,6*α*-epoxy-3*β*-ol (**3**),[9] a known coisolate from this species, both the absolute configurations of C-20 and C-24 were assigned as *R*.

Finally, the absolute configuration of **1** was determined by means of ECD and optical rotation calculations on two possible structures: (3*S*,5*R*,6*S*,7*R*,8*S*,10*S*,13*R*,14*R*,17*R*,20*R*,24*R*)-**1** (**1a**) and (3*R*,5*S*,6*R*,7*S*,8*R*,10*R*,13*S*,14*S*,17*S*,20*R*,24*R*)-**1** (**1b**) (Supporting Information).[10] Overall, conformation searches on **1a** and **1b** by the MMFF94s force field give 18 and 16 conformers

Table 1. ^1H NMR (500 MHz) and ^{13}C NMR (125 MHz) Spectroscopic Data of Matsutakone (1) (δ in ppm)

no.	δ_H [a]	δ_C [a]	δ_H [b]	δ_C [b]
1*β*	1.79, ddd (13.5, 4.8, 2.5)	29.3, CH_2	2.15, overlapped	30.8
1*α*	1.76, dd (13.5, 3.9)		2.10, overlapped	
2*β*	1.64, overlapped	30.1, CH_2	2.26, m	31.5
2*α*	2.00, overlapped		2.00, m	
3	3.97, m	68.6, CH	4.47, m	68.3
3-OH			6.44, br. s	
4*β*	1.49, dd (12.5, 7.0)	38.1, CH_2	1.84, overlapped	39.5
4*α*	2.12, dd (12.5, 11.0)		2.48, dd (12.5, 11.0)	
5		68.8, C		69.8
6	3.21, d (4.0)	62.8, CH	3.39, d (4.0)	63.7
7	2.20, m	48.0, CH	2.58, m	49.5
8		76.0, C		75.9
8-OH	1.87, s			
9		211.1, C		213.0
10		46.3, C		47.2
11*β*	1.75, overlapped	24.6, CH_2	2.10, overlapped	25.7
11*α*	1.75, overlapped		1.83, overlapped	
12*β*	1.91, ddd (12.6, 3.6, 3.6)	39.2, CH_2	1.94, ddd (12.8, 3.6, 3.6)	40.1
12*α*	1.22, ddd (12.6, 12.6, 6.0)		1.28, ddd (13.0, 13.0, 4.0)	
13		43.4, C		43.9
14	1.46, overlapped	59.0, CH	1.87, overlapped	60.3
15*β*	2.12, overlapped	19.3, CH_2	2.66, m	20.9
15*α*	1.46, overlapped		1.99, m	
16*β*	1.37, m	28.3, CH_2	1.46, m	29.1
16*α*	1.69, m		1.74, m	
17	1.15, dd (19.5, 9.5)	56.8, CH	1.20, dd (19.5, 9.5)	57.2
18	0.68, s	14.0, CH_3	0.99, s	14.9
19	1.51, s	22.4, CH_3	1.77, s	23.4
20	2.01, m	40.0, CH	2.06, m	40.8
21	0.99, d (6.5)	21.0, CH_3	1.05, d (6.5)	21.5
22	5.14, dd (15.0, 8.5)	135.5, CH	5.20, dd (15.0, 7.9)	136.5
23	5.22, dd (15.0, 8.0)	132.3, CH	5.26, dd (15.0, 7.0)	132.4
24	1.84, m	43.0, CH	1.87, m	43.4
25	1.46, m	33.2, CH	1.47, m	33.7
26	0.82, d (7.0)	19.8, CH_3	0.85, d (6.7)	20.2
27	0.83, d (7.0)	20.1, CH_3	0.86, d (6.7)	20.5
28	0.91, d (7.0)	17.8, CH_3	0.94, d (6.8)	18.2

[a]Recorded in $CDCl_3$. [b]Recorded in C_5D_5N.

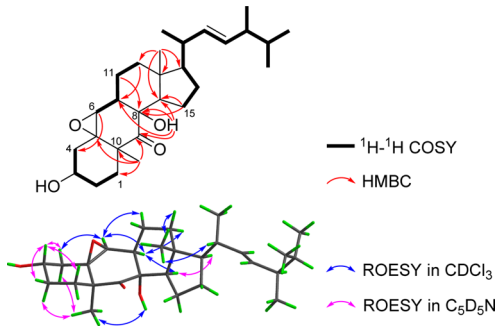

Figure 2. Key 2D NMR correlations of **1**.

DOI: 10.1021/acs.joc.7b01230
J. Org. Chem. 2017, 82, 7974−7979

with population higher than 1%, respectively. All of these conformers were optimized at the B3LYP/6-31G(d,p) of theory to give eight and seven conformers within a 3 kcal/mol energy threshold from global minimum, respectively. These predominant conformers were subjected to theoretical calculation of ECD using time-dependent density functional theory (TDDFT) at B3LYP/6-31G(d,p) level in gas phase with PCM model. As shown in Figure 3, the calculated ECD spectrum of **1a** matched well with the experimental one, suggesting the absolute configuration of **1** to be 3*S*,5*R*,6*S*,7*R*,8*S*,10*S*,13*R*,14*R*,17*R*,20*R*,24*R* (Figure 3).

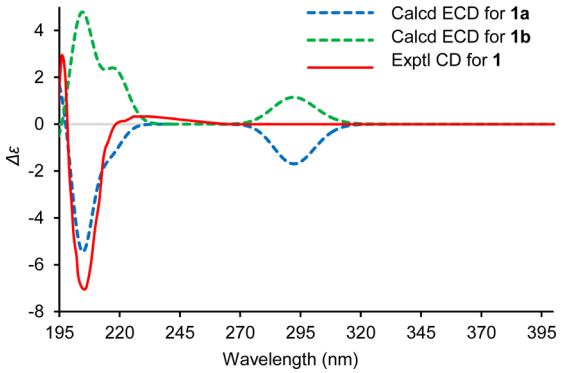

Figure 3. Comparison of the calculated ECD spectra for **1a** and **1b** with the experimental spectrum of **1** in MeCN.

The specific optical rotations ($[\alpha]_D$) of the two possible structures (3*S*,5*R*,6*S*,7*R*,8*S*,10*S*,13*R*,14*R*,17*R*,20*R*,24*R*)-**1** and (3*R*,5*S*,6*R*,7*S*,8*R*,10*R*,13*S*,14*S*,17*S*,20*R*,24*R*)-**1** were calculated at the B3LYP/6-311++g(2d,p) level with PCM model in MeCN based on predominant B3LYP/6-311g(2d,p) optimized geometries.[11] The calculated specific rotation (+53.6°) of (3*S*,5*R*,6*S*,7*R*,8*S*,10*S*,13*R*,14*R*,17*R*,20*R*,24*R*)-**1** was close to the experimental value ($[\alpha]_D^{21}$ +12.9, *c* 0.14, MeCN), while the calculated data for (3*R*,5*S*,6*R*,7*S*,8*R*,10*R*,13*S*,14*S*,17*S*,20*R*,24*R*)-**1** ($[\alpha]_D$ −35.5) had opposite sign to the experimental value (pages S40, S41, Supporting Information). Therefore, the results of specific optical rotation calculations suggest same conclusion with the ECD calculation results.

Given that matsutakone (**1**) harbored an unprecedented carbon skeleton, the calculations of ^{13}C NMR chemical shifts of (3*S*,5*R*,6*S*,7*R*,8*S*,10*S*,13*R*,14*R*,17*R*,20*R*,24*R*)-**1** at the mPW1PW91/6-311++g(2d,p) level with PCM model in $CHCl_3$ based on predominant B3LYP/6-311g(2d,p) optimized geometries were performed (pages S41−S43, Supporting Information).[12] The results revealed that the correlation coefficient (R^2) between the calculated and experimental data from linear regression analysis was 0.9989 with the largest outlier $\Delta\delta$ = 3.3 ppm (C-10), and the root-mean-square deviation (RMSD) was 1.45 ppm, which further provided solid evidence for the structural rationality of **1** (Figure 4).

The colorless oil matsutoic acid (**2**) possessd the molecular formula $C_{18}H_{30}O_3$ with four degrees of unsaturation on the basis of HRMS (ESI-TOF) data (*m*/*z*: [M + Na]$^+$ calcd for $C_{18}H_{30}O_3$ 317.2087; found 317.2092). The ^{1}H NMR together with HSQC and HMBC spectra of **2** displayed resonances attributable to four methyl doublets (δ_H 0.82, 0.84, 0.93, 1.08) and one methyl singlet (δ_H 0.95) as well as two coupling olefinic protons [δ_H 5.21, dd (*J* = 15.0, 8.7 Hz); 5.31, dd (*J* = 15.0, 7.8 Hz)]. The ^{13}C and DEPT spectra showed signals for

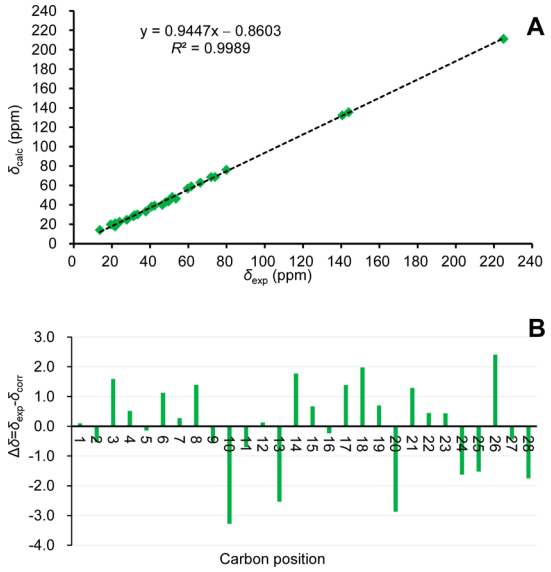

Figure 4. (A) Regression analysis of experimental versus calculated ^{13}C NMR chemical shifts of **1** at mPW1PW91/6-311++g(2d,p) level; linear fitting was shown as a line. (B) Relative chemical shift errors between scaled ^{13}C NMR and experimental ^{13}C NMR for **1** (δ_{corr} obtained by linear fit δ_{exp} versus δ_{calcd}).

four methylene, six methine, and three quaternary carbons (a keto group, a carboxy group) (Table 2). All the functional groups accounted for three degrees of unsaturation, and the remaining one degree of unsaturation suggested that **2** possessed only one ring.

The planar structure of **2** was deduced by extensive analyses of the 2D NMR spectra and were described as follows. The ^{1}H−^{1}H COSY spectroscopic data between H-11/H-10/H-12/

Table 2. ^{1}H NMR (500 MHz) and ^{13}C NMR (125 MHz) Spectroscopic Data of Matsutoic Acid (2) (δ in ppm)

	2 ($CDCl_3$)	
no.	δ_H	δ_C
1		178.6, C
2	2.41, m	29.6, CH_2
	2.16, m	
3	2.06, m	32.0, CH_2
	1.81, m	
4		51.2, C
5		223.4, C
6	2.32, dd (18.0, 8.7)	37.4, CH_2
	2.07, overlapped	
7	2.00, overlapped	24.0, CH_2
	1.49, overlapped	
8	1.78, m	47.9, CH
9	0.95, s	17.9, CH_3
10	2.22, m	38.9, CH
11	1.08, d (6.5)	21.0, CH_3
12	5.21, dd (15.0, 8.7)	133.3, CH
13	5.31, dd (15.0, 7.8)	134.4, CH
14	1.89, m	43.1, CH
15	1.49, m	33.2, CH
16	0.82, d (7.0)	19.8, CH_3
17	0.84, d (7.0)	20.1, CH_3
18	0.93, d (7.0)	17.7, CH_3

DOI: 10.1021/acs.joc.7b01230
J. Org. Chem. 2017, 82, 7974−7979

H-13/H-14/H-15/H-16 as well as H-14/H-18, H-15/H-17, H-8/H-10 revealed the presence of a typical steroid side chain (Figure 5). Futhermore, the obvious HMBC correlations from

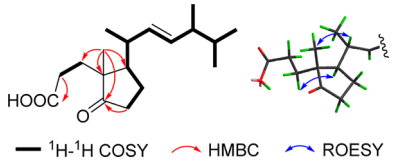

Figure 5. Key 2D NMR correlations of **2**.

Me-9 (δ_H 0.95) to C-3 (δ_C 32.0), C-4 (δ_C 51.2), C-5 (δ_C 223.4), C-8 (δ_C 47.9), from H-6 (δ_H 2.32, 2.07) to C-5, along with the ^{1}H−^{1}H COSY correlations between H-6/H-7/H-8 enabled the completion of the five-membered ring. Besides, ^{1}H−^{1}H COSY correlations between H-2/H-3 and HMBC correlations from H-2 (δ_H 2.41, 2.16) to C-1 (δ_C 178.6) suggested the presence of the other side chain (C1−C2−C3) connected at C-4. All this evidence prompted the establishment of the planar structure of **2**.

The geometry of the Δ^{12} double bond was determined as *E* form based on the large coupling constant between H-12 and H-13 (J = 15.0 Hz), and the absolute configurations of C-20 and C-24 were assigned as *R* by comparing the chemical shifts with **1**. The relative configurations of C-4 and C-8 of **2** were established as 4*R**,8*R** by ROESY correlations of H-3/H-8 and Me-9/H-10. To establish the absolute configurations of **2**, the specific optical rotations ($[\alpha]_D$) of the two possible structures (4*R*,8*R*)-**2** and (4*S*,8*S*)-**2** were calculated at the B3LYP/6-311++g(2d,p) level with PCM model in MeOH based on predominant B3LYP/6-311g(2d,p) optimized geometries (pages S43−S45, Supporting Information).[11] The calculated specific rotation (−79.3) of (4*R*,8*R*)-**2** was close to the experimental value ($[\alpha]_D^{22}$ −47.3, *c* 0.10, MeOH), while the calculated data for (4*S*,8*S*)-**2** ($[\alpha]_D$ +40.7) had opposite sign to the experimental value.

Matsutakone (**1**) and matsutoic acid (**2**) represented (nor)steroids with unprecedented carbon skeletons, which aroused our interest in their plausible biogenesis. Biosynthetically, compounds **1** and **2** might possibly be traced back to the normal ergosterol since they possessed the common side chain. The postulated biogenetic pathways for **1** and **2** were proposed (Scheme 1). The co-isolated compound 5,6-epoxy-22-en-3-ol-ergosterol (**3**)[9] was oxygenated at C-7, C-8 double bond and C-9 to give the key intermediate **H** which possessed an epoxy group. The intermediate **H** followed by an oxidative cleavage between C-9 and C-11 in basic condition to give **I**. The plane of rings A and B of **I** underwent a 180° rotation, providing advantageous conditions for a vital nucleophilic addition reaction from C-11 carbanion to C7-C8-epoxy to yield compound **1**. On the other hand, compound **3** underwent an oxidative cleavage between C-7 and C-8 to give intermediate **J**, which further yielded the key intermediate **K** in basic condition. Oxidative cleavage of intermediate **K** between the double bond of enol group gave intermediate **L**, which further underwent a decarboxylative reaction and an oxidation process to give compound **2**.

Since neurodegenerative diseases like Alzheimer's disease caused by decrease of acetylcholine (ACh) content threaten the quality of life of the aged, we have evaluated the anti-AChE activities of **1** and **2** by the method as previously reported.[13] In the experiment, tacrine (TA) was used as positive control. The results showed that **1** and **2** exhibited inhibition rates of 62.8% and 40.3% at the concentration 50 μM, respectively. The IC_{50} value of **1** was 20.9 μM (Table 3).

Table 3. Inhibitory Activities Against AChE of 1 and 2

samples	TA	1	2
concentration (μM)	0.333	50	50
inhibition rate (%)	58.0 ± 1.08	62.8 ± 0.38	40.3 ± 1.73
IC_{50} (μM)	0.20	20.9	–

Scheme 1. Proposed Biosynthetic Pathways for 1 and 2

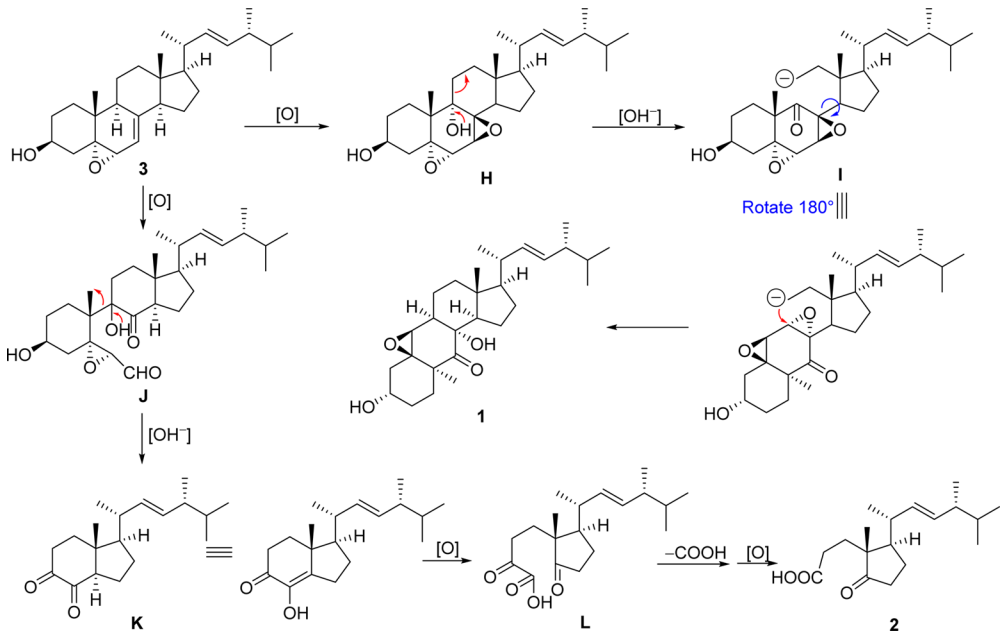

DOI: 10.1021/acs.joc.7b01230
J. Org. Chem. 2017, 82, 7974−7979

In summary, chemical investigations on the famous edible mushroom of *T. matsutake* were carried out, which resulted in the isolation of a sterol matsutakone (**1**) bearing a previously undescribed scaffold and a new norsteroid matsutoic acid (**2**). Their structures were unambiguously determined via extensive spectroscopic analysis in combination with computational approaches. Moreover, anti-AChE bioassay results suggested that ingesting fruiting bodies of *T. matsutake* was beneficial to human health.

EXPERIMENTAL SECTION

General Experimental Procedures. Optical rotation was obtained on a JASCO P-1020 digital polarimeter. UV spectrum was recorded on a Shimadzu UV-2401PC. CD spectrum was measured on an Applied Photophysics Chirascan Circular Dichroism Spectrometer. IR spectrum was taken on a Bruker Tensor 27 FT-IR spectrometer. 1D and 2D NMR spectra were obtained on a Bruker Ascend 500 MHz and a Bruker Avance III 600 MHz spectrometers. HRESIMS data were measured on an Agilent 6200 Q-TOF MS system . Silica gel (Qingdao Haiyang Chemical Co., Ltd.) was used for normal column chromatography (CC). Medium-pressure liquid chromatography (MPLC) was performed on a Büchi Sepacore System equipped with pump manager C-615, pump modules C-605, and fraction collector C-660, and columns packed with Chromatorex C-18 (40−75 μm). Preparative high-performance liquid chromatography (prep-HPLC) was performed on an Agilent 1260 liquid chromatography system equipped with a Zorbax SB-C18 column (5 μm, 9.4 mm × 150 mm, 7 mL·min^{-1}) and a DAD detector.

Fungal Material. The fruiting bodies *Tricholoma matsutake* were purchased from Nyingchi, Tibetan Autonomous Region in June 2014 and identified by Prof. Yu-Cheng Dai (Beijing Forestry University), who is an expert in the field of mushroom taxonomy. A voucher specimen of *T. matsutake* was deposited in the Herbarium of Kunming Institute of Botany, Chinese Academy of Sciences (no. HFC 20140626).

Extraction and Isolation. The air-dried and powdered fruiting bodies of *T. matsutake* (2.0 kg) were soaked with 95% ethanol for three times. The extract was evaporated under reduced pressure and partitioned between ethyl acetate and water for four times to give a crude extract (25 g). The crude extract was subject to normal CC with a stepwise gradient of petroleum ether/acetone (v/v 10:1−1:1) to afford four fractions (A−C).

Fraction B (6.0 g) was subjected to MPLC with a gradient solvent system of MeOH/H_2O (v/v 20:80−100:0, 25 mL·min^{-1}) to obtain 17 subfractions (B1−B17). Subfraction B5 (30 mg), B10 (35 mg), and B4 (24 mg) was further purified by Sephadex LH-20 (eOH), followed by prep-HPLC to yield compound **1** (1.4 mg, MeCN-H_2O: 60%−75%, 20 min, 7 mL·min^{-1}, t_R = 16.2 min), **2** (2.5 mg, MeCN-H_2O: 30%−65%, 35 min, 7 mL·min^{-1}, t_R = 31.1 min), and **3** (5.5 mg, MeCN-H_2O: 70%−90%, 25 min, 7 mL·min^{-1}, t_R = 8.5 min).

*Matsutakone (**1**).* Amorphous white powder; $[\alpha]_D^{21}$ +12.9 (*c* 0.14, MeCN); UV (MeCN) λ_{max} (log ε) 196 (4.03) nm; IR (KBr) ν_{max} 3433, 2958, 2931, 2872, 1631, 1383 cm^{-1}; HRMS (ESI-TOF) *m*/*z*: $[M + Na]^+$ calcd for $C_{28}H_{44}O_4Na$ 467.3132; found 467.3121.

*Matsutoic Acid (**2**).* Colorless oil; $[\alpha]_D^{22}$ −47.3 (*c* 0.10, MeOH); UV (MeOH) λ_{max} (log ε) 230 (2.29) nm; IR (KBr) ν_{max} 3434, 2964, 2927, 2878, 1732, 1628, 1384 cm^{-1}; HRMS (ESI-TOF) *m*/*z*: $[M + Na]^+$ calcd for $C_{18}H_{30}O_3Na$ 317.2087; found 317.2092.

Acetylcholinesterase Inhibitory Activity Assay. Acetylcholinesterase (AChE) inhibitory activity of compounds **1** and **2** was assayed by the spectrophotometric method developed by Ellman et al.[13] with slightly modification. *S*-Acetylthiocholine iodide, *S*-butyrylthiocholine iodide, 5,5′-dithio-bis(2-nitrobenzoic) acid (DTNB, Ellman's reagent), acetylcholinesterase derived from human erythrocytes were purchased from a chemical supplier. Compound **1** was dissolved in DMSO. The reaction mixture (totally 200 μL) containing phosphate buffer (pH 8.0), test compound (50 μM), and acetyl cholinesterase (0.02 U/mL) was incubated for 20 min (37 °C). Then, the reaction was initiated by the addition of 40 μL of solution containing DTNB (0.625 mM) and acetylthiocholine iodide (0.625 mM) for AChE inhibitory activity assay, respectively. The hydrolysis of acetylthiocholine was monitored at 405 nm every 30 s for 1 h. Tacrine was used as positive control with final concentration of 0.333 μM. All of the reactions were performed in triplicate. The percentage inhibition was calculated as follows: inhibition rate (%) = $(E - S)/E \times 100$ (E is the activity of the enzyme without test compound and S is the activity of enzyme with test compound).

ECD Calculation. The ECD calculations for compounds (3*S*,5*R*,6*S*,7*R*,8*S*,10*S*,13*R*,14*R*,17*R*,20*R*,24*R*)-**1** (**1a**) and (3*R*,5*S*,6*R*,7*S*,8*R*,10*R*,13*S*,14*S*,17*S*,20*R*,24*R*)-**1** (**1b**) were performed using Gaussian 09. Conformation searches based on molecular mechanics with MMFF94s force field were performed for **1a** and **1b** and gave 18 and 16 conformers with populations higher than 1%.[10] All of these conformers were further optimized by the density functional theory (DFT) method at the B3LYP/6-31G(d,p) level in Gaussian 09 program package[10c] and led to eight (**1aA**-**1aH**) and seven (**1bA**-**1bG**) conformers for **1a** and **1b** within a 3 kcal/mol energy threshold from global minimum, respectively (Supporting Information). These predominant conformers were subjected to theoretical calculation of ECD using time-dependent density functional theory (TDDFT) at B3LYP/6-31G(d,p) level in air with PCM model. The calculated ECD curves for **1a** and **1b** and weighted ECD were all generated using SpecDis 1.60 with σ = 0.15 eV and UV shift −10 nm, respectively.[14]

Specific Optical Rotation Calculation. The specific optical rotation calculations for compounds (3*S*,5*R*,6*S*,7*R*,8*S*,10*S*,13*R*,-14*R*,17*R*,20*R*,24*R*)-**1** (**1a**) and (3*R*,5*S*,6*R*,7*S*,8*R*,10*R*,13*S*,14*S*,17*S*,20*R*,24*R*)-**1** (**1b**) were performed using Gaussian 09 (Supporting Information). The conformers **1aA**-**1aH** and **1bA**-**1bG** were further optimized at the B3LYP/6-311G(2d,p) level in gas phase to give the respective conformers **1aAA**-**1aHA** and **1bAA**-**1bGA**, all of which were subjected to specific optical rotation calculations at the B3LYP/6-311+G(2d,p) level in MeCN with PCM model. The calculated specific optical rotation data of these conformers were averaged according to the Boltzmann distribution theory and their relative Gibbs free energy.

^{13}C NMR Calculation. Gauge-independent atomic orbital (GIAO) calculations of ^{13}C NMR of conformers **1aAA**-**1aHA** were accomplished by DFT at the mPW1PW91/6-311++g(2d,p) level in $CHCl_3$ with PCM model in Gaussian 09 software package (Supporting Information). The ^{13}C NMR chemical shift was calculated in the same level and used as references. The calculated NMR data of these conformers were averaged according to the Boltzmann distribution theory and their relative Gibbs free energy. Compared to the experimental data, linear correlation coefficients (R^2) and root-mean-square deviation (RMSD) were calculated for evaluation of the results.

ASSOCIATED CONTENT

Supporting Information

The Supporting Information is available free of charge on the ACS Publications website at DOI: 10.1021/acs.joc.7b01230.

Spectroscopic data including 1D &2D NMR, HRMS, UV, IR, optical rotations, and calculation details of **1** and **2** (PDF)

AUTHOR INFORMATION

Corresponding Authors

*E-mail: tfeng@mail.scuec.edu.cn.

*E-mail: jkliu@mail.kib.ac.cn.

ORCID

Bin Wu: 0000-0001-6048-4965

Tao Feng: 0000-0002-1977-9857

Author Contributions

⊥These authors contributed equally to this work.

DOI: 10.1021/acs.joc.7b01230
J. Org. Chem. 2017, 82, 7974−7979

Notes

The authors declare no competing financial interest.

■ ACKNOWLEDGMENTS

This work was financially supported by National Key Technology Support Program, China (2013BAI11B02), National Natural Science Foundation of China (81561148013), and the Key Projects of Technological Innovation of Hubei Province (No. 2016ACA138). The authors thank Analytical & Measuring Center, School of Pharmaceutical Sciences, and South-Central University for Nationalities for MS and NMR spectra tests. The computational work was supported by HPC Center, Kunming Institute of Botany, CAS, China.

■ REFERENCES

(1) (a) Liu, J. K. *Chem. Rev.* **2005**, *105*, 2723−2744. (b) Liu, J. K. *Chem. Rev.* **2006**, *106*, 2209−2223. (c) Zhou, Z. Y.; Liu, J.-K. *Nat. Prod. Rep.* **2010**, *27*, 1531−1570. (d) Jiang, M. Y.; Feng, T.; Liu, J. K. *Nat. Prod. Rep.* **2011**, *28*, 783−808.

(2) (a) Liu, D. Z.; Wang, F.; Liao, T. G.; Tang, J. G.; Steglich, W.; Zhu, H. J.; Liu, J. K. *Org. Lett.* **2006**, *8*, 5749−5752. (b) Chen, H. P.; Zhao, Z. Z.; Li, Z. H.; Dong, Z. J.; Wei, K.; Bai, X.; Zhang, L.; Wen, C. N.; Feng, T.; Liu, J. K. *ChemistryOpen* **2016**, *5*, 142−149.

(3) (a) Schlegel, B.; Härtl, A.; Dahse, H.-M.; Gollmick, F. A.; Gräfe, U. *J. Antibiot.* **2002**, *55*, 814−817. (b) Porco, J. A.; Su, S.; Lei, X.; Bardhan, S.; Rychnovsky, S. D. *Angew. Chem., Int. Ed.* **2006**, *45*, 5790−5792. (c) Sekizawa, R.; Ikenon, S.; Nakamura, H.; Naganawa, H.; Matsui, S.; Iinuma, H.; Takeuchi, T. *J. Nat. Prod.* **2002**, *65*, 1491−1493.

(4) Wu, J.; Tokuyama, S.; Nagai, K.; Yasuda, N.; Noguchi, K.; Matsumoto, T.; Hirai, H.; Kawagishi, H. *Angew. Chem., Int. Ed.* **2012**, *51*, 10820−10822.

(5) (a) Hao, J. *Shipin Gongye Keji.* **2011**, *32*, 213−214. (b) Hu, J.; Liu, J. *Shipin Gongye (Shanghai, China)* **2011**, *32*, 107−109.

(6) Luan, H. Y.; Wang, G. Y.; Yang, M. *Anhui Nongye Kexue.* **2012**, *40*, 8471−8472.

(7) Zhang, Y.; Li, J.; Liu, L. S.; Chen, L. H. *Shipin Gongye Keji.* **2016**, *37*, 156−160.

(8) (a) Gawas, D.; Garcia, R.; Huch, V.; Müller, R. *J. Nat. Prod.* **2011**, *74*, 1281−1283. (b) Wang, S.; Zhang, L.; Liu, L. Y.; Dong, Z. J.; Li, Z. H.; Liu, J. K. *Nat. Prod. Bioprospect.* **2012**, *2*, 240−244.

(9) Kang, J.; Wang, H. Q.; Chen, R. Y. *Int. J. Med. Mushrooms* **2003**, *5*, 391−396.

(10) (a) Goto, H.; Osawa, E. *J. Am. Chem. Soc.* **1989**, *111*, 8950−8951. (b) Goto, H.; Osawa, E. *J. Chem. Soc., Perkin Trans. 2* **1993**, 187−198. (c) Frisch, M. J.; Trucks, G. W.; Schlegel, H. B.; Scuseria, G. E.; Robb, M. A.; Cheeseman, J. R.; Scalmani, G.; Barone, V.; Mennucci, B.; Petersson, G. A.; Nakatsuji, H.; Caricato, M.; Li, X.; Hratchian, H. P.; Izmaylov, A. F.; Bloino, J.; Zheng, G.; Sonnenberg, J. L.; Hada, M.; Fukuda, R.; Hasegawa, J.; Ishida, M.; Nakajima, T.; Honda, Y.; Kitao, O.; Nakai, H.; Vreven, T.; Montgomery, J. A., Jr.; Ogliaro, F.; Bearpark, M.; Heyd, J. J.; Brothers, E.; Kudin, K. N.; Staroverov, V. N.; Keith, T.; Kobayashi, R.; Normand, J.; Raghavachari, K.; Rendell, A.; Burant, J. C.; Iyengar, S. S.; Tomasi, J.; Cossi, M.; Rega, N.; Millam, J. M.; Klene, M.; Knox, J. E. J.; Cross, B.; Bakken, V.; Adamo, C.; Jaramillo, J.; Gomperts, R.; Stratmann, R. E.; Yazyev, O.; Austin, A. J.; Cammi, R.; Pomelli, C.; Ochterski, J. W.; Martin, R. L.; Morokuma, K.; Zakrzewski, V. G.; Voth, G. A.; Salvador, P.; Dannenberg, J. J.; Dapprich, S.; Daniels, A. D.; Farkas, O.; Foresman, J. B.; Ortiz, J. V.; Cioslowski, J.; Fox, D. J. *Gaussian 09*, revision C.01; Gaussian, Inc.: Wallingford, CT, 2010.

(11) Stephens, P. J.; Devlin, F. J.; Cheeseman, J. R.; Frisch, M. J. *J. Phys. Chem. A* **2001**, *105*, 5356−5371.

(12) Lodewyk, M. W.; Tantillo, D. J. *J. Nat. Prod.* **2011**, *74*, 1339−1343.

(13) Ellman, G. L.; Courtney, K. D.; Andres, V. J.; Featherstone, R. M. *Biochem. Pharmacol.* **1961**, *7*, 88−95.

(14) Bruhn, T.; Schaumlöffel, A.; Hemberger, Y.; Bringmann, G. *Spec Dis*, version 1.60; University of Würzburg: Würzburg, Germany, 2012.

DOI: 10.1021/acs.joc.7b01230
J. Org. Chem. 2017, 82, 7974−7979